Article

Design and Synthesis of a Thermally Stable Organic Electride

Mikhail Y. Redko, James E. Jackson, Rui H. Huang, and James L. Dye

J. Am. Chem. Soc., **2005**, 127 (35), 12416-12422• DOI: 10.1021/ja053216f • Publication Date (Web): 10 August 2005

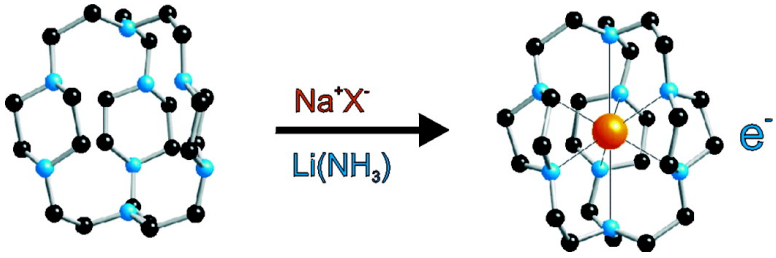

More About This Article

Additional resources and features associated with this article are available within the HTML version:

- Supporting Information
- Links to the 9 articles that cite this article, as of the time of this article download
- Access to high resolution figures
- Links to articles and content related to this article
- Copyright permission to reproduce figures and/or text from this article

View the Full Text HTML

J|A|C|S
ARTICLES
Published on Web 08/10/2005

Design and Synthesis of a Thermally Stable Organic Electride

Mikhail Y. Redko,[†] James E. Jackson,[†] Rui H. Huang,[†] and James L. Dye*[,†,‡]

Contribution from the Department of Chemistry, Michigan State University, East Lansing, Michigan 48824, and SiGNa Chemistry, LLC, 530 East 76th Street, Suite 9E, New York, New York 10021

Received May 17, 2005; E-mail: dye@msu.edu

Abstract: An electride has been synthesized that is stable to auto-decomposition at room temperature. The key was the theoretically directed synthesis of a per-aza analogue of cryptand[2.2.2] in which each of the linking arms contains a piperazine ring. This complexant was designed to provide strong complexation of Na^+ via pre-organization of a "crypt" that contains eight nonreducible tertiary amine nitrogens. The structure and properties indicate that, as with other electrides, the "anions" are electrons trapped in the cavities formed by close-packing of the complexed cations. The isostructural sodide, with Na^- anions in the cavities, is also stable at and above room temperature.

Introduction

Organic *electrides* are crystalline salts in which alkali cations (Li^+ through Cs^+) are complexed by organic molecules that serve to isolate the cations from electrons trapped in intermolecular cavities and channels.[1−7] Electrides provide unique examples of low-density electron gases confined to cavities and channels of known geometry, which makes them related to both salts and plasmas. Therefore, they are of interest in theories of electron−spin interactions and the insulator−metal transition. Because the electrons are weakly bound, electrides also exhibit low-energy electron emission[8,9] that could be useful in devices such as IR-sensitive photomultipliers and thermoelectric power or refrigeration sources. Thermal instability above about −40 °C of the seven previously synthesized electrides that contain oxa-based complexants presented major difficulties in their study and use. For example, electrides made with crown ethers and cryptands, such as cryptand[2.2.2] (**1**), spontaneously decomposed at ambient temperatures to ethylene and an alkoxide.[10] Here we describe the design, synthesis, structure, and properties of an electride and a sodide that are stable (in the absence of air and moisture) to this destructive process up to and above room temperature.

When alkali metals can be dissolved in pure or mixed amine or ether solvents without a complexant, such solutions generally contain, in addition to alkali cations, both solvated electrons (e^-_{solv}) and alkali metal anions (M^-).[11,12] Removal of the solvent, or the addition of a less polar solvent, results in re-formation of the metal. The addition of a powerful complexant for alkali metal cations, such as a cryptand, a crown ether, or an aza analogue, greatly increases metal solubility by complexing the cations, and prevents re-formation of the metal upon solvent removal.

The synthesis of pure electrides rather than mixtures with alkalides requires suppression of the concentration of alkali metal anions in solution. In favorable cases, a slight excess of a strong enough complexant, L, for the cations can suppress alkali metal anion formation through the reaction,

$$M^- + L \rightleftharpoons M^+L + 2e^-_{solv} \quad (1)$$

For a given solvent, the equilibrium position of reaction 1 depends on both the alkali metal and the complexant. At one extreme, Li^- has never been observed in solution, while Na^- is so thermodynamically favored in amines and ethers that, until the present work, no electride with Na^+L as the cation had been synthesized.

The previous synthesis of a thermally stable sodide and a potasside[13] exploited the ability of the fully methylated aza-cryptand, **2**, to complex K^+. Its thermal stability confirmed earlier conclusions that tertiary nitrogen aza analogues of crown ethers and cryptands are robust toward reductive bond cleavage. For example, sodides that contained Li^+ in a smaller aza-cryptand[14] and those that had K^+ or Cs^+ complexed by an aza-crown ether[15] were stable to decomposition at and above room

[†] Michigan State University.
[‡] SiGNa Chemistry, LLC.

(1) Dawes, S. B.; Ward, D. L.; Huang, R. H.; Dye, J. L. *J. Am. Chem. Soc.* **1986**, *108*, 3534−3535.
(2) Dye, J. L. *Prog. Inorg. Chem.* **1984**, *32*, 327−441.
(3) Dye, J. L. *Nature* **1993**, *365*, 10−11.
(4) Dye, J. L.; Wagner, M. J.; Overney, G.; Huang, R. H.; Nagy, T. F.; Tomanek, D. *J. Am. Chem. Soc.* **1996**, *118*, 7329−7336.
(5) Dye, J. L. *Inorg. Chem.* **1997**, *36*, 3816−3826.
(6) Dye, J. L. *Science* **2003**, *301*, 607−608.
(7) Wagner, M. J.; Dye, J. L. In *Molecular Recognition: Receptors for Cationic Guests*, 1st ed.; Gokel, G. W., Ed.; Pergamon Press: Oxford, U.K., 1996; Vol. 1, pp 477−510.
(8) Huang, R. H.; Dye, J. L. *Chem. Phys. Lett.* **1990**, *166*, 133−136.
(9) Phillips, R. C.; Dye, J. L. *Chem. Mater.* **2000**, *12*, 3642−3647.
(10) Cauliez, P. M.; Jackson, J. E.; Dye, J. L. *Tetrahedron Lett.* **1991**, *32*, 5039−5042.
(11) Matalon, S.; Golden, S.; Ottolenghi, M. *J. Phys. Chem.* **1969**, *73*, 3098−3101.
(12) DeBacker, M. G.; Dye, J. L. *J. Phys. Chem.* **1971**, *75*, 3092−3096.
(13) Kim, J.; Ichimura, A. S.; Huang, R. H.; Redko, M.; Phillips, R. C.; Jackson, J. E.; Dye, J. L. *J. Am. Chem. Soc.* **1999**, *121*, 10666−10667.
(14) Eglin, J. L.; Jackson, E. P.; Moeggenborg, K. J.; Dye, J. L.; Bencini, A.; Micheloni, M. *J. Inclusion Phenom.* **1992**, *12*, 263−274.
(15) Kuchenmeister, M. E.; Dye, J. L. *J. Am. Chem. Soc.* **1989**, *111*, 935−938.

10.1021/ja053216f CCC: $30.25

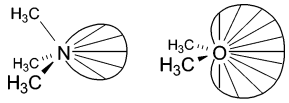

Figure 1. Effective angular ranges for Na^+ binding to methylamine (μ = 0.61 D,[18] ±45°) and dimethyl ether (μ = 1.31 D,[19] ±75°). These angles correspond to those that yield two-thirds of the axial (maximal) binding energy in each case. Line lengths in the diagrams correspond to association energies computed at the corresponding angles.

temperature. However, none of these complexants yielded a crystalline electride.

Better aza complexants for Na^+ and K^+ would have preformed cages with nitrogen lone-pairs that point toward the encapsulated cation. Little conformational change from that of the free complexant would minimize the energy and entropy costs associated with reorganization. Space-filling (CPK) models and calculations suggested that incorporation of six-membered piperazine rings in the three connecting arms of an aza-cryptand would provide a complexant **3** (abbreviated TriPip222)[16] with better pre-organization than that which is present in the hexamethylated complexant **2**.

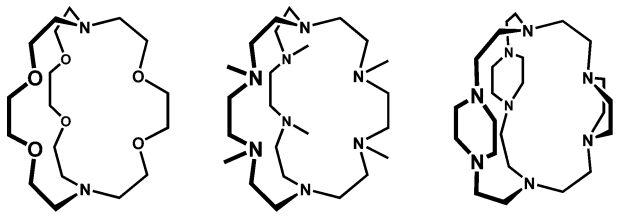

1 **2** **3**

Results and Discussion

Theory. The synthesis of TriPip222 cryptand, **3**, was based on a design strategy that sought a ligand with the complexing ability of the classical [2.2.2] or [2.2.1] cryptands,[17] but without the ether linkages that had proven vulnerable to electron capture and reductive cleavage in previous electrides and alkalides.[10] Simple orbital reasoning, confirmed by electronic structure calculations, suggested that decreasing the coordinating heteroatom electronegativity by replacing oxygen with nitrogen would raise the complexants' LUMO energies enough to make them inaccessible for the electron attachment that leads to thermal decomposition of oxa-based complexants. The design of suitable aza complexants must overcome two problems: (1) with their lower dipole moments, aliphatic tertiary amine nitrogen sites are intrinsically weaker ligands for alkali metals than are ether oxygens, and (2) the range of effective orientations for M^+ coordination by an amine, with its single nonbonding electron pair, is smaller than that for an ether, which offers two lone pairs. The effective angular ranges for coordination, as calculated for the gas-phase model donors trimethylamine and dimethyl ether, are illustrated in Figure 1.

The need to predict the ability of complexants to bind alkali cations before embarking on long and complicated syntheses prompted a theoretical analysis of the factors involved in such complexation. Could peraza complexants be designed with binding energies comparable to those of cryptands? The ligands **1**−**3** and their Na^+ complexes were modeled via ab initio calculations at two levels. Preliminary candidate structures for input to the quantum chemical modeling packages were generated by using the structure building and MMX molecular mechanics force field available in the PCModel software[20] running on a dual-1GHz processor Macintosh G4. Additional starting geometries for optimizations were generated from X-ray structural coordinates.[13,21,22] The few lowest energy conformations of complexants and their Na^+ complexes were geometry-optimized at the RHF/3-21G level of theory. The program suites Gaussian 98,[23] Gaussian 03,[24] and GAMESS[25] running on various platforms were used. Subsequent re-optimizations at the B3LYP/6-311+G(d) level were then performed. The higher level calculations used Gaussian 98 running on a 32-processor Silicon Graphics Origin 3400 at Michigan State University and Gaussian 03 running on the multiprocessor facilities at the Pittsburgh Supercomputer Center. Numerous checks to verify the consistency of results across software packages and hardware platforms were performed, and all of the final B3LYP/6-311+G(d) calculations were carried out with Gaussian 03 on the Pittsburgh Supercomputing Center "Rachel" cluster.

Augmented by insights from about 60 crystal structures in the Cambridge Data Base[26] that contain Na^+·**1**, as well as prior conformational studies,[27−29] these calculations made it clear that both **1** and **2** are quite "floppy" and lack pre-organized binding pockets. Instead, they undergo "induced fits" to achieve the optimal geometry for ion complexation. The amount of structural reorganization required by **2** for cation binding is similar to that in **1**, but, because of the geometrical differences between ether and amine coordination sites described above, its conformational rearrangement is more energetically costly. This factor, and the intrinsically weaker $N-M^+$ binding energy compared with that of $O-M^+$, explain the modest performance of **2** as a ligand for alkali metal cations.

The pentacyclic ligand **3** offers a natural solution to the weaknesses of **2**. By "tying together" the sterically demanding methyl groups of **2**, the strain of organizing and pulling in the six closest nitrogen atoms about the metal center is lowered. In addition, the entropy decrease associated with organizing the complexant for cation binding is presumably smaller, which would make the net free energy of binding more negative. Meanwhile, the three diamine straps of the cage consist of piperazine rings which, in their twist-boat conformations, naturally orient the nitrogen lone pair sites toward the bound metal cation. As can be seen for the free ligand in Figure 2C, the cyclohexane-like piperazine rings prefer the chair conformation. In fact, however, the calculated chair-boat inversion

(16) IUPAC name: 1,4,7,10,13,16,21,24-octaazapentacyclo[8.8.8.24,7.213,-16.221,24]dotriacontane.
(17) Lehn, J.-M. *Struct. Bonding (Berlin)* **1973**, *16*, 1−70.

(18) Lide, D. R.; Mann, D. E. *J. Chem. Phys.* **1958**, *28*, 572−576.
(19) Blukis, U.; Kasai, P. H.; Myers, R. J. *J. Chem. Phys.* **1963**, *38*, 2753−2760.
(20) *PCMODEL*, version 8.0; Serena Software, Box 3076, Bloomington, IN 47402-3076.
(21) Tehan, F. J.; Barnett, B. L.; Dye, J. L. *J. Am. Chem. Soc.* **1974**, *96*, 7203−7208.
(22) Allen, F. H. *Acta Crystallogr.* **2002**, *B58*, 380−388.
(23) Frisch, M. J.; et al. *Gaussian 98*, version SCI64-G98, revision A.11; Gaussian, Inc.: Pittsburgh, PA, 1998.
(24) Frisch, M. J.; et al. *Gaussian 03*, version MacOSX-G03, revision B.04; version A164T-G03, revision C.01; Gaussian, Inc: Pittsburgh, PA, 2004.
(25) Schmidt, M. W.; et al. *J. Comput. Chem.* **1993**, *14*, 1347−1363.
(26) Allen, F. H.; Motherwell, W. D. S. *Acta Crystallogr.* **2002**, *B58*, 407−422.
(27) Geue, R.; Jacobson, S. H.; Pizer, R. *J. Am. Chem. Soc.* **1986**, *108*, 1150−1155.
(28) Troxler, L.; Wipff, G. *J. Am. Chem. Soc.* **1994**, *116*, 1468−1480.
(29) Adam, K. R.; Atkinson, I. M.; Kim, J.; Lindoy, L. F.; Matthews, O. A.; Meehan, G. V.; Raciti, F.; Skelton, B. W.; Svenstrup, N.; White, A. H. *J. Chem. Soc., Dalton Trans.* **2001**, 2388−2397.

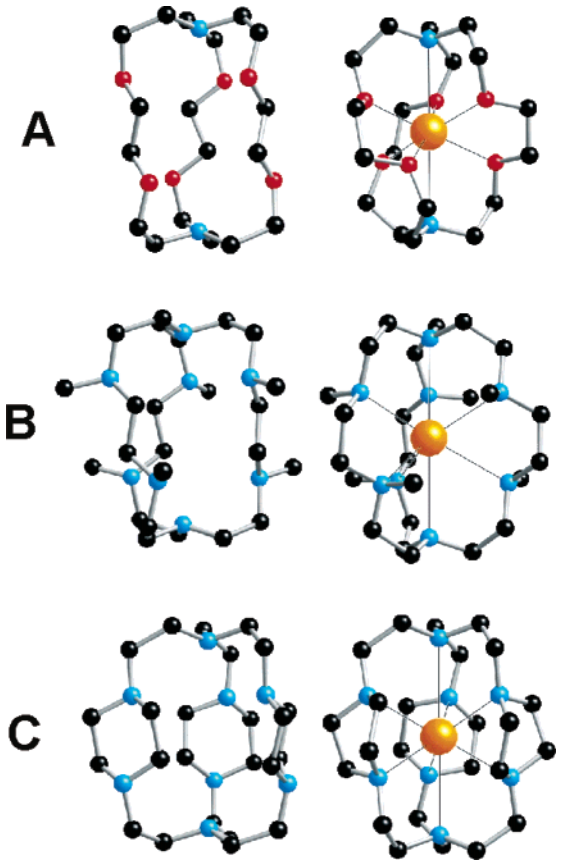

Figure 2. Comparison of the structures of the three empty ligands and their corresponding Na^+ complexes. Row A displays the structures for cryptand[2.2.2] (**1**) and its Na^+ complex. Row B shows those of the permethylated peraza [2.2.2] analogue (**2**), and row C gives those of the TriPip222 aza-cryptand (**3**). The diagrams shown were obtained from crystal structures where available. Except for small differences for free **1**, the calculated structures of all species are indistinguishable by eye from the X-ray structures.

energies for three free *N*,*N*′-dimethylpiperazine rings (3 × 38 kJ/mol) substantially exceed the 77 kJ/mol energy difference between the ligand in the binding geometry and the relaxed empty ligand. This value compares with rearrangement energies of 85 kJ/mol for cryptand[2.2.2] (**1**) and 91 kJ/mol for **2**. Despite the larger conformational energy cost incurred by **1**, the calculated overall binding energy of Na^+, −418 kJ/mol, is greater than those of **3** (−392 kJ/mol) and **2** (−367 kJ/mol). These calculations show that the weaker binding of Na^+ by **2** than by either **1** or **3** results primarily from the energy of the conformational change, probably augmented by a larger entropy decrease. As a result of these calculations, the aza-cryptand **3** became the target of synthesis.

The structures of the three free ligands and their Na^+ complexes are shown in Figure 2. The crystal structures of **3** and the electride, Na^+**·3**·e^-, are considered later (Table 1). Confidence in the validity of the gas-phase calculations is gained by the fact that, in all cases, the calculated structures are virtually identical to those obtained from crystal structures where available. For example, the calculated N−Na^+ distances are only slightly longer than those observed for four salts that contain Na^+**·3** (Table 2).

Synthesis. The synthesis of **3** is outlined in Scheme 1. The aza-cryptand[2.2.2] (**4**) was synthesized in multigram amounts

Table 1. Crystal Structure Data (Å)

	electride	sodide	TriPip222
crystal system	orth	orth	orth
space group	*Pccn*	*Pccn*	*Pbca*
unit cell			
a (Å)	10.703(2)	11.074(2)	18.149(4)
b (Å)	14.608(3)	14.812(3)	20.315(4)
c (Å)	18.606(4)	18.825(4)	27.882(6)
α, *β*, *γ* (deg)	90	90	90
volume (Å^3)	2909.1(10)	3087.8(11)	10280(4)
Z	8	8	8
R for $I > 2\sigma$	0.1110	0.1463	0.1270
largest diff. peak	0.486/−0.197	0.174/−0.224	0.243/−0.290

Table 2. Experimental and Calculated N−Na^+ Distances (Å)

N position	Na^+**·3**·e^-	Na^+**·3**·Na^-	Na^+**·3**·ClO_4^-	Na^+**·3**·AQS$^-$	Na^+**·3** (calcd)
top	3.059	3.041	3.083	3.056	3.091
bottom	3.059	3.041	3.080	3.093	3.091
strand 1	2.633	2.637	2.642	2.621	2.739
	2.633	2.637	2.675	2.623	2.739
strand 2	2.636	2.645	2.670	2.640	2.739
	2.652	2.650	2.642	2.703	2.739
strand 3	2.652	2.650	2.641	2.671	2.739
	2.636	2.645	2.645	2.677	2.739

Scheme 1

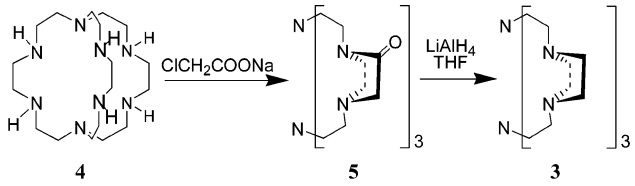

4 **5** **3**

by a one-pot modification[30] of the synthesis reported by Smith et al.[31] The complexing ability of **3** for Na^+ is so strong that it is difficult to avoid inadvertent encapsulation of sodium ion during synthesis. Because the rate of complexation of Na^+ is slow at the low temperatures used in electride synthesis, Na^+ was pre-encapsulated with a "sacrificial anion", and the electride and sodide were formed by a metathesis reaction similar to that used to prepare "inverse sodium hydride".[32]

Successful metathesis requires an anion that is able to form an ammonia-soluble salt with the complexed cation and that reacts with lithium metal in ammonia and/or methylamine to form an insoluble salt plus solvated electrons. (Sodium rather than lithium is used for the synthesis of sodides.) The large size and hydrophobic exterior of complexed cations yield a low solvation energy in liquid ammonia. As a result, most of the complexed salts M^+LA^- are not soluble enough in liquid ammonia to provide good yields of the electride. During the preparation of protonated adamanzane sodide, we had used nitrate, glycolate, and isethionate as sacrificial anions.[32] All of these salts had very low solubilities in liquid ammonia, and the yield of $AdzH^+Na^-$ was typically only about 6%. In the present work, none of these anions provided enough solubility of the Na^+(TriPip222) salt to be used for electride synthesis.

The first electride samples were made with 2-anthraquinone

(30) Redko, M. Y.; Jackson, J. E.; Dye, J. L. *Synthesis* **2005**, submitted; U.S. Patent Appl. 10/866,858, 2005.
(31) Smith, P. H.; Barr, M. E.; Brainard, J. R.; Ford, D. K.; Freiser, H.; Muralidharan, S.; Reilly, S. D.; Ryan, R. R.; Silks, L. A., III; Yu, W. *J. Org. Chem.* **1993**, *58*, 7939−7941.
(32) Redko, M. Y.; Vlassa, M.; Jackson, J. E.; Misiolek, A. W.; Huang, R. H.; Dye, J. L. *J. Am. Chem. Soc.* **2002**, *124*, 5928−5929.

sulfonate (AQS^-, **6**) as the anion. This anion has a large hydrophobic group, making it easy to extract the salt Na^+(TriPip222)AQS^- from an aqueous solution with dichloromethane for purification by chromatography. The salt was purified, its crystal structure was determined, and its reaction with Li in liquid ammonia yielded an electride, but in low yield (<10%). The electride and sodide crystal structures and some properties were determined from these early preparations. However, the low solubility of Na^+(TriPip222)AQS^- in liquid ammonia made the synthetic procedure difficult to carry out and hard to reproduce.

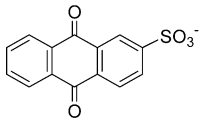

6

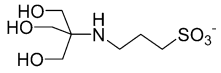

7

After testing a number of anions, we found that 3-[tris-(hydroxymethyl)methylamino]-1-propanesulfonate (**7**, abbreviated $TAPS^-$) had the desired properties of solubility and reducibility. This anion is much more flexible than those used previously and probably uses its three hydroxyl groups to form hydrogen bonds with ammonia. These features make Na^+(TriPip222)$TAPS^-$ highly soluble in liquid ammonia, and the reduction of the hydroxyl groups by reaction with dissolved lithium forms an insoluble lithium salt (with the evolution of hydrogen). After removal of ammonia by vacuum evaporation, dimethyl ether (Me_2O) was added to dissolve the electride, and the solution was filtered into the product side of a K-cell.[2] Lithium and sodium are insoluble in Me_2O, so excess metal remains in the synthesis side of the K-cell. Vacuum evaporation of the dimethyl ether, followed by washing with trimethylamine and final removal of all solvents by evacuation to $\sim 10^{-5}$ Torr, gave the desired electride as a black powder in >50% yield.

Crystal Structures. The crystal structures of TriPip222 (**3**), Na^+·**3**·ClO_4^-, Na^+·**3**·AQS^-, Na^+·**3**·Na^-, and Na^+·**3**·e^- were all determined. The crystal structure data for free **3** and the electride and sodide are presented in Table 1, and the CIF files for all of the structures are given in the Supporting Information. The structure of the complexed cation, Na^+·**3**, is essentially the same in the four compounds, as reflected by the N−Na^+ distances listed in Table 2. The sodide and electride are isostructural, with only minor changes in the inter-ionic distances. This reinforces the concept that electrons act as anions in electrides, with the electron density concentrated in the cavities formed by packing of the complexed cations.[4−6] In the free complexant, the six-membered rings of the three strands are in chair conformations. Formation of the Na^+ complex involves conversion to the boat conformation, which results in the orientation of all nitrogen lone pairs toward the cation at the center of the complex.

Electride Properties. The optical spectra of thin films of the electride and sodide are shown in Figure 3. The films were formed by dissolving powder samples in Me_2O, producing a thin liquid film on the walls of the optical cell, and rapidly evaporating the solvent.[33] The optical peak at 1450 nm is typical of electrides, while the 670 nm peak is that of Na^-. Note that the electride film contained a small amount of sodide. These thin films underwent slow decomplexation at and above room temperature to form the sodide.

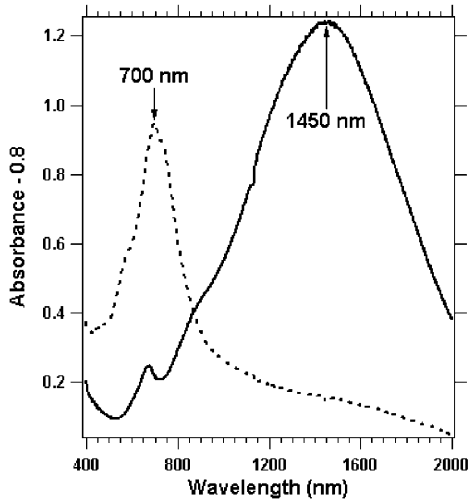

Figure 3. Optical spectra of thin films of Na^+(TriPip222)e^- (solid) and Na^+(TriPip222)Na^- (dotted). Solvent-free films were formed by rapid evaporation of dimethyl ether from liquid films of the appropriate solution on the walls of an optical cell.[34] The baseline has been displaced by 0.8 absorbance unit because of light-scattering by the solid film.

The magnetic and electrical properties of electrides depend primarily on the nature of the channels that connect the trapping cavities. The inter-electron spin coupling (*J*-value) increases dramatically from one electride to another as the channel diameter increases.[4,5] The electrides studied to date, including Na^+·**3**·e^-, have their largest channels oriented along one direction. As a result, the temperature dependence of the magnetic susceptibility follows the 1D Heisenberg chain model. The molar susceptibility for such systems can be described by the analytic expression[35] obtained from the calculations of Bonner and Fisher[36] for a 1D chain of spins,[37] (plus a

$$\chi_m = \frac{Ng^2\beta^2}{kT}\left[\frac{0.25 + 0.14995x + 0.30094x^2}{1 + 1.9862x + 0.68854x^2 + 6.0626x^3}\right] \quad (2)$$

diamagnetic term), in which $x = |J|/kT$. The magnetic susceptibility of Na^+·**3**·e^- as a function of temperature is shown in Figure 4. The behavior is similar to that of other electrides except for the extended temperature range that could be studied. The fit to the 1D Heisenberg chain model is excellent with $J/k_B = -11.1 \pm 0.05$ K. Because of air-sensitivity, the sample mass of only 14 mg was determined by difference after the experiment. Weighing errors of a few milligrams are difficult to avoid because of possible loss of glass fragments upon breaking the Suprasil sample tube, removal of material upon cleaning the empty tube, etc. If the apparent mass of 14 mg is used, the magnitude of the susceptibility corresponds to only 71% of that expected for this mass of a pure electride. The optical spectra and ^{23}Na NMR spectra obtained from the same preparation rule out the presence of enough sodide to cause this discrepancy. The diamagnetic contribution also suggests a weighing error.

(33) Dye, J. L.; Yemen, M. R.; DaGue, M. G.; Lehn, J.-M. *J. Chem. Phys.* **1978**, *68*, 1665−1670.
(34) DaGue, M. G.; Landers, J. S.; Lewis, H. L.; Dye, J. L. *Chem. Phys. Lett.* **1979**, *66*, 169−172.
(35) Estes, W. E.; Gavel, D. P.; Hatfield, W. E.; Hodgson, D. *Inorg. Chem.* **1978**, *17*, 1415−1421.
(36) Bonner, J. C.; Fisher, M. E. *Phys. Rev. A* **1964**, *135*, 640−658.
(37) Wagner, M. J.; Ichimura, A. S.; Huang, R. H.; Phillips, R. C.; Dye, J. L. *J. Phys. Chem. B* **2000**, *104*, 1078−1087.

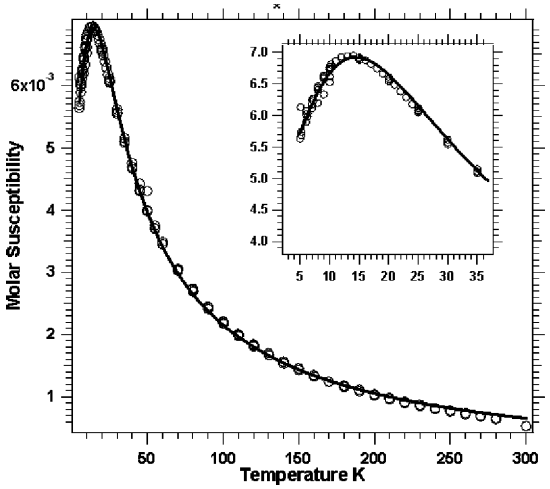

Figure 4. Molar magnetic susceptibility of $Na^+(TriPip222)e^-$ as a function of temperature. The solid line is a fit to the Heisenberg 1D chain model with $J/k_B = -11.1$ K. The data shown are for four temperature scans. The inset shows the behavior near the susceptibility maximum.

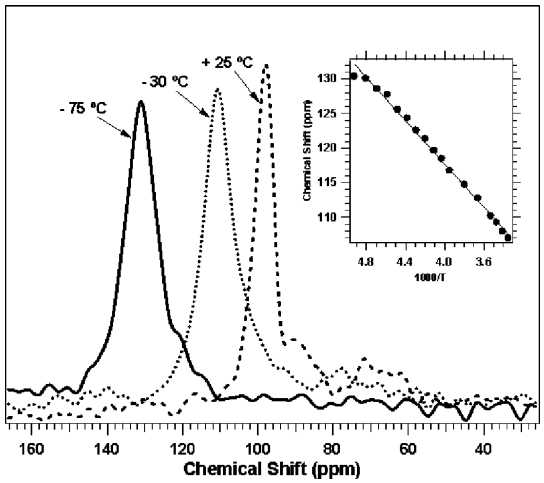

Figure 5. ^{23}Na MAS NMR spectra of $Na^+(TriPip222)e^-$ in the low-temperature region. The single peak shifts smoothly over the temperature range from −80 to +25 °C as a result of the Knight shift, a measure of the unpaired electron density at the Na^+ nucleus. There are no other peaks in this temperature range. All chemical shifts are relative to $Na^+(aq)$ at 25 °C.

The apparent mass (14 mg) leads to the unreasonably low value of only -196×10^{-6} emu/mol, compared with -321×10^{-6} emu/mol calculated by using the Pascal constants[38] for Na^+**·3**. Correction to a mass of 0.71 × 14 mg yields $-(276 \pm 20) \times 10^{-6}$ emu/mol.

The ^{23}Na MAS NMR spectra as a function of temperature provide much information about the nature of the electride and the decomplexation processes. As shown in Figure 5, the peak shifts smoothly with an increase in temperature between −80 and +30 °C. This Knight shift[39] gives a measure of the unpaired electron contact density at the Na^+ nucleus through the equation

$$K(T) = (8\pi/3N)\,\langle|\psi(0)|^2\rangle\,\chi(T) \qquad (3)$$

in which $\langle|\psi(0)|^2\rangle$ is the average unpaired electron density at the nucleus, $\chi(T)$ is the molar magnetic susceptibility, and N is Avogadro's number. In the temperature region of interest, $\chi(T)$ is linear in $1/T$, so $K(T)$ is also, as shown in the inset to Figure 5. Combination of the two sets of data yields $\langle|\psi(0)|^2\rangle = 5 \times 10^{21}$ cm^{-3} for the average unpaired electron density at Na^+ in the electride. Comparison with the unpaired electron density at the free Na atom (5×10^{24} cm^{-3})[40] yields only 0.1% atomic character for the complexed sodium cation. This is consistent with the low values for other electrides.[41,42] The MAS NMR line width is constant at ∼1100 Hz between −80 and 0 °C, and then it decreases to a constant value of ∼600 Hz at 20 °C before conversion to the peaks of Na^+ and Na^- at 35 °C. This rapid decrease in line width probably results from a change in the average electric field gradient when the complexant undergoes thermally activated conformational changes or rotation above about 20 °C.[43]

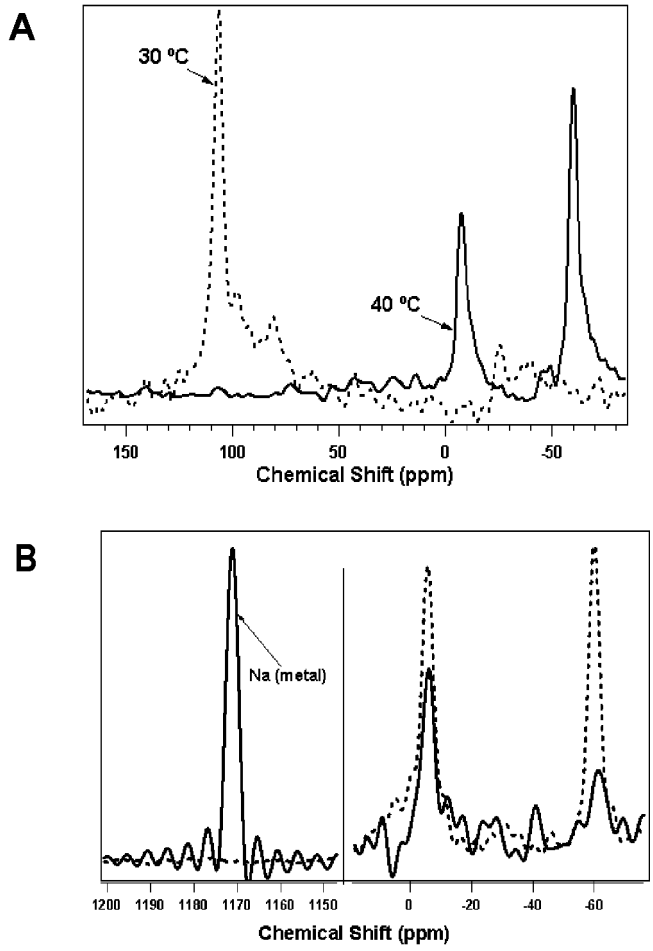

Figure 6. Changes in the ^{23}Na MAS NMR spectra of the electride, $Na^+(TriPip222)e^-$, with temperature. (A) Conversion of the shifted peak of the electride at 30 °C to the two peaks of the sodide, $Na^+(TriPip222)Na^-$, at 40 °C. (B) Conversion of the resulting sodide at 100 °C (dotted) to sodium metal at 110 °C (solid). Note that the peak of Na^- is nearly gone at 110 °C, but that some complexed Na^+ remains.

As the temperature approaches +40 °C, dramatic changes in the ^{23}Na MAS NMR spectra occur. As shown in Figure 6A,

(38) Selwood, P. W. *Magnetochemistry*; Interscience: New York, 1943.
(39) Knight, W. D. *Phys. Rev.* **1944**, *76*, 1259−1260.
(40) O'Reilly, D. E. *J. Chem. Phys.* **1964**, *41*, 3729−3735.
(41) Dawes, S. B.; Ellaboudy, A. S.; Dye, J. L. *J. Am. Chem. Soc.* **1987**, *109*, 3508−3513.
(42) Dawes, S. B.; Eglin, J. L.; Moeggenborg, K. J.; Kim, J.; Dye, J. L. *J. Am. Chem. Soc.* **1991**, *113*, 1605−1609.
(43) Wagner, M. J.; McMills, L. E. H.; Ellaboudy, A. S.; Eglin, J. L.; Dye, J. L.; Edwards, P. P.; Pyper, N. C. *J. Phys. Chem.* **1992**, *96*, 9656−9660.

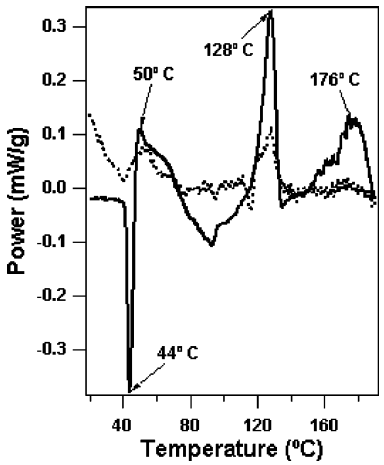

Figure 7. DSC of Na^+(TriPip222)e^- (solid) and Na^+(TriPip222)Na^- (dotted) as functions of temperature.

the peak of complexed Na^+ that is paramagnetically shifted by the unpaired electrons disappears, and peaks due to Na^+ in the complex (−8 ppm) and to Na^- (−60 ppm) appear. These changes occur because the electride is converted to the sodide by decomplexation of half of the complexed Na^+, which reacts with electrons to form Na^-. The peaks of complexed Na^+ and free Na^- persist unshifted up to 110 °C, at which temperature the balance of the Na^+ decomplexes and reacts with Na^- to form sodium metal with its characteristic large Knight shift of 1170 ppm[39] (Figure 6B). The processes that occur are summarized by the following equations:

$$2Na^+(TriPip222)e^- \rightarrow Na^+(TriPip222)Na^- + TriPip222 \quad (\text{at } 40\ ^\circ C)$$

$$\rightarrow 2Na(liq.) + 2TriPip222 \quad (\text{at } 110\ ^\circ C) \quad (4)$$

The ^{23}Na MAS NMR spectra of the sodide, Na^+(TriPip222)Na^- (not shown), have only the peaks of complexed Na^+ and free Na^- near −12 and −68 ppm, respectively. These are the only peaks observed at −60, −40, +25, and +50 °C, and the chemical shifts are temperature independent, as expected for diamagnetic samples. At +99 °C an additional peak due to metallic sodium appears at 1160 ppm. Thus, as shown for the electride after conversion to the sodide, the latter is stable to about 100 °C. The temperature independence of the intensity of the sodide NMR peak relative to that of Na^+ up to 100 °C shows that the complexant is remarkably resistant to reduction, even under these severe conditions.

Differential scanning calorimetry (DSC) traces of the electride and the sodide are shown in Figure 7. There is a sharp endotherm at +44 °C in the DSC trace of the electride (ΔH = +19 J/g), followed immediately by a broad exotherm (ΔH = −44 J/g). These results are consistent with the ^{23}Na MAS NMR behavior described above. Both the DSC and NMR data indicate that at 40−45 °C the electride is converted to a mixture of the sodide and free complexant. The sharp DSC endotherm, followed by an exotherm, indicates that decomplexation of Na^+ occurs, followed by the exothermic reaction of Na^+ with e^- to form Na^-. The decomplexation then stops, leaving half of the complexant free of Na^+. Starting at about 100 °C, an exotherm in the DSC (ΔH = −43 J/g) corresponds to the conversion of Na^+**·3·**Na^- to the free complexant plus Na(liquid), just as was observed in the ^{23}Na MAS NMR spectrum.

The DSC results for the sodide (Figure 7) also agree with the NMR results and show that Na^+**·3·**Na^- is stable toward both decomposition and decomplexation up to about 100 °C.

Conclusions

We have known for some time that the stability of alkalides and electrides to irreversible thermal decomposition required replacement of oxygen by nitrogen in the complexants used. But, since aza-based complexants provide weaker binding of alkali metal cations than their oxa counterparts, compensation is required in the form of a reduced conformational energy contribution. According to theory, the proposed complexant, TriPip222 (**3**), met this requirement, and its synthesis and the subsequent preparation of a thermally stable electride verified the theoretical predictions.

Now that a stable molecular architecture for complexation has been found, the opportunities for elaboration abound. The substitution of K^+ for Na^+ in the complexant may provide an electride with greater thermal stability against decomplexation. The addition of various groups to the carbon atoms in the arms should result in changes in packing and in the geometry of the electron-trapping cavities and the connecting channels. If these sidearms contain aromatic groups, they may provide additional electron-trapping sites, providing the ability to study competition between cavity-trapping and molecule-trapping. Finally, the ability to handle organic electrides at and above room temperature will make the study of electride properties much simpler.

Experimental Section

Solvent purification, alkali metal handling, and general synthesis techniques have been described previously.[44]

Na^+(TriPip222)ClO_4^-. A mixture of 4.42 g of **4**·4H_2O (10 mmol) and 4.66 g of $ClCH_2COONa$ (40 mmol, 33% excess) was refluxed in 50 mL of 1-butanol in a 100 mL round-bottom flask for 12 h in a nitrogen atmosphere. The butanol was then evaporated in a N_2 stream, the resulting mixture was redissolved in 50 mL of 2-propanol and filtered, and the 2-propanol was evaporated to yield a crude oily mixture of polyamides. After addition of 2.0 g of $LiAlH_4$ and 50 mL of fresh THF to the mixture, it was refluxed for 12 h in a nitrogen atmosphere. After the mixture was cooled, excess $LiAlH_4$ was quenched by dropwise addition of 10 mL of saturated aqueous NaOH and 20 mL of 2-propanol. The resulting mixture was refluxed for 3 h and yielded two immiscible liquid phases. The top phase, containing **3**, was poured onto a solution of 5 mL of saturated aqueous $NaClO_4$ and refluxed for 5 min, and then slowly cooled and filtered, and the precipitate of Na^+**·3·**ClO_4^- was rinsed with cold water and dried on the filter. Yield: 2.85 g (50%, based on **4**). The crystals of Na^+**·3·**ClO_4^- were grown by hexane diffusion into its $CDCl_3$ solution. ***CAUTION! Organic perchlorates can be explosive and should be handled with care and not heated when dry.***

^{1}H NMR (300 MHz, $CDCl_3$): δ 2.089 (b), 2.533 (b), 2.780 (b), 3.042 (b). ^{13}C NMR (300 MHz, $CDCl_3$): δ 49.348, 49.606, 54.857. ^{23}Na NMR: δ −9.646 (relative to NaC222Br−$CDCl_3$ at δ = −14.491 ppm).

TriPip222. Na^+**·3·**ClO_4^- (0.3 g) was refluxed with 1.5 mL of 70% $HClO_4$ in 10 mL of *i*-PrOH for 1 d; the **3·**n$HClO_4$ precipitate was filtered, rinsed with *i*-PrOH, and dried on the filter. The precipitate was dissolved in 30 mL of H_2O and treated with 10 mL of 10%

(44) Dye, J. L. *J. Phys. Chem.* **1984**, *88*, 3842−3846.

$Me_4N^+OH^-$ (Aldrich), and the released **3** was extracted from the suspension of $Me_4N^+ClO_4^-$ with 5 × 10 mL of $CDCl_3$.

^1H NMR (300 MHz, $CDCl_3$): δ 2.429 (b, 10H), 2.717 (b, 38 H). ^{13}C NMR (300 MHz, $CDCl_3$): δ 50.683, 50.881, 52.505. Anal. Calcd for $C_{24}H_{48}N_8$: C, 64.24; H, 10.78; N, 24.97. Found: C, 62.75; H, 10.59; N, 24.10. Crystals of TriPip222 were grown by slow evaporation of a pentane solution at ~ −10 °C.

Na^+(TriPip222)AQS$^-$. A mixture of 3.7 g of **4**·$4H_2O$ (8.37 mmol) was refluxed with 4.0 g of $ClCH_2COONa$ (34 mmol) in 50 mL of 1-butanol overnight, and then the solution was filtered into a 100 mL flask and the solvent evaporated. The product was reduced with 2.0 g of $LiAlH_4$ in refluxing THF overnight, solid pellets of NaOH (4.0 g) were added to the reaction mixture, and the excess $LiAlH_4$ was quenched with 50% aqueous 2-propanol upon reflux. As a result, two phases were formed in the flask: the dense one contained mostly water and inorganic salts, while the light one consisted mostly of THF, 2-propanol, and dissolved polyamines. The reaction mixture was cooled to room temperature, the bottom phase solidified, and the top phase was poured into a different flask. The solvents were then evaporated, 3.1 g of sodium anthraquinone sulfonate monohydrate (9.44 mmol, Aldrich) and 30 mL of H_2O were added, and the mixture was refluxed for 30 min. The solution was cooled to room temperature, the excess of sodium anthraquinone sulfonate was filtered off, and Na^+·**3**·AQS^- was extracted with 2 × 50 mL of CH_2Cl_2. The solvent was then removed with a rotary evaporator, and then, within 3 days, the obtained melt crystallized to yield crystals of Na^+·**3**·AQS^-·CH_2Cl_2. One of the crystals was selected for crystal structure determination; the rest of the material was purified by chromatography on silica (eluent, 70% CH_2Cl_2−30% EtOH). Evaporation of the solvent gave a crystalline material that was used for the initial synthesis of sodium TriPip222 sodide and electride.

^1H NMR (300 MHz, $CDCl_3$): δ 2.041 (b), 2.552 (b), 2.770 (b) and 3.018 (b, 48H, N−C**H**$_2$), 7.751 (m, 2H), 8.254 (mt, 3H), 8.378 (1H, AB quadruplet, J_1 = 8 Hz, J_2 = 1.8 Hz), 8.844 (1H, d, J = 1.8 Hz). ^{13}C NMR (300 MHz, $CDCl_3$): δ 49.378, 49.621, 54.978, 125.551, 127.084, 127.144, 132.213, 133.230, 133.822, 133.928.

Na^+(TriPip222)TAPS$^-$·CH_2Cl_2. A mixture of the amides (2.0 g), obtained by the reaction of **4** with $ClCH_2COONa$, was refluxed with 2.0 g of $LiAlH_4$ in 50 mL of THF, cooled to 0 °C, and quenched with saturated aqueous NaOH. The THF solution of **3** was poured off the viscous mixture of inorganic compounds, the solvent was evaporated, and the resulting oil was refluxed overnight with 1.2 g of H^+TAPS^- (Acros Organics) and 2.0 g of Na_2CO_3 in 40 mL of EtOH. The solution was filtered, and the ethanol was evaporated to yield an oil that was rinsed with 50 mL of C_6H_6. This led to crystallization of Na^+·**3**·$TAPS^-$. The product was redissolved in CH_2Cl_2, and the solution was filtered and evaporated. Yield: 0.98 g (34%).

^1H NMR (300 MHz, $CDCl_3$): δ 5.260 (2H, CH_2Cl_2), 3.475 (s, 6H, CH_2OH), 2.972 (t, J = 7.2 Hz), 2.821 (t, J = 7.2 Hz), 2.016 (q, J = 7.2 Hz) on top of a large broad hump δ = 1.5−3.15 (69H, calcd 58H). ^{13}C NMR (300 MHz, $CDCl_3$): δ 63.310 (**C**H_2OH), 59.698 (**C**$(CH_2OH)_3$), 54.978 (ligand), 53.821 (CH_2Cl_2), 49.621 (ligand), 49.378 (ligand), 47.785 (NH−**C**H_2), 38.041 (**C**H_2−SO_3^-), 25.626 (CH_2**C**H_2CH_2).

Na^+(TriPip222)Na$^-$. A solution of 0.14 g of Na^+·**3**·AQS^-·CH_2Cl_2 (0.17 mmol) in 5 mL of EtOH was added to the synthesis side of a standard K-cell, and the solvent was removed by evacuation. The resulting solid was dissolved in 5 mL of $MeNH_2$ at 0 °C with the aid of sonication for 30 min. The solution was cooled to −78 °C and the $MeNH_2$ was pumped out, resulting in the formation of a solid foam of poorly crystallized Na^+·**3**·AQS^-. Na (92 mg) was then added to the cell in a He-filled drybox so that the piece of sodium fell into a tube that connected the reaction and product sides of the K-cell, thus avoiding direct contact with the salt. The salt was then dissolved in 5 mL of $MeNH_2$ at 0 °C, the solution was cooled to −78 °C (no precipitation took place at this point), and the piece of Na was dropped into the solution. No reaction occurred until 10 mL of NH_3 was condensed onto the reaction mixture, which resulted in a formation of a dark-blue methylamine solution with golden droplets of Na−NH_3 phase floating on top. The solvents were pumped off and 5 mL of Me_2O was condensed onto the product mixture, which resulted in a dark-blue solution of Na^+·**3**·Na^- in this solvent. The solution was filtered through a frit into the product side of the K-cell, and golden crystals of Na^+(TriPip222)Na^- were grown by slow cooling (−50 to −75 °C) of a solution in a dimethyl ether−trimethylamine mixture.

Vis−near-IR: λ = 698 nm.

Na^+(TriPip222)e$^-$. Na^+·**3**·$TAPS^-$·CH_2Cl_2 (0.268 g) was dissolved in 10 mL of EtOH, and the solution was put into a K-cell. The solvent was evaporated under vacuum, and the solid was redissolved in 10 mL of EtOH, which was evaporated again. Next, 5 mL of NH_3 was condensed onto the salt at −78 °C, the solution was transferred through a frit to the product compartment, and the solvent was evaporated. Lithium (40 mg) was loaded into the reaction side of the cell in a He-filled glovebox, and then both Na^+·**3**·$TAPS^-$ and Li were dissolved in NH_3 at −78 °C. The Na^+·**3**·$TAPS^-$ solution was poured onto the Li solution, and NH_3 was removed by evacuation at −78 °C for 1 week. Dimethyl ether (5 mL) was condensed onto the product mixture and evaporated under vacuum three times. After that, 5 mL of fresh Me_2O was condensed onto the product mixture, and the dark-blue electride solution was filtered through the frit to the product side of the cell. The Me_2O was then distilled back onto the product mixture three times to dissolve all of the electride, followed each time by filtration to the product side. Finally, Me_3N (2 mL) was condensed into the Me_2O solution, and the solvents were removed by evacuation overnight at −78 °C. The electride powder was rinsed with fresh Me_3N (4 mL) three times, Me_3N was evaporated under vacuum, and the cell was broken, while cold, in a nitrogen-filled glovebag. Samples of the cold electride powder were loaded into an optical cell, MAS NMR rotor, and a SQUID tube. Crystals were grown by slow cooling (−50 to −75 °C) of a solution of the electride in a mixture of dimethyl ether and diethyl ether.

Acknowledgment. We are grateful for assistance with synthesis by Jonathon J. Brudnak and with NMR studies by Kermit Johnson. This work was supported in part by NSF Grant DMR 9988881.

Supporting Information Available: Complete lists of authors for refs 23−25 (PDF); crystallographic data of five compounds that contain **3** (CIF). This material is available free of charge via the Internet at http://pubs.acs.org.

JA053216F